Thresholds for Perceiving Changes in Friction When Combined With Linear System Dynamics

Veldhuis, Robbin; Mulder, Max; van Paassen, M. M.

DOI
10.1109/THMS.2024.3368358

Publication date
2024

Document Version
Final published version

Published in
IEEE Transactions on Human-Machine Systems

Citation (APA)
Veldhuis, R., Mulder, M., & van Paassen, M. M. (2024). Thresholds for Perceiving Changes in Friction When Combined With Linear System Dynamics. *IEEE Transactions on Human-Machine Systems*, *54*(3), 260-270. https://doi.org/10.1109/THMS.2024.3368358

Thresholds for Perceiving Changes in Friction When Combined With Linear System Dynamics

Robbin Veldhuis, Max Mulder, *Senior Member, IEEE*, and M. M. van Paassen, *Senior Member, IEEE*

***Abstract*—Understanding human perception of haptic feedback is critical when designing and regulating these interfaces. In recent years, experiments have been conducted to determine the just-noticeable difference (JND) in mass–spring–damper dynamics, using a hydraulic admittance display in the form of a side-stick. These experiments have resulted in a model of JNDs when interacting with linear second-order dynamics. In real-world applications, however, control force dynamics also commonly include nonlinearities, such as friction. This research extends the current understanding of JNDs in linear systems by including the nonlinear case, where friction is also present. Experiments were conducted to determine JNDs in friction when combined with second-order system dynamics. Results indicate that friction JND can be independent of linear system dynamics as long as its value compared to the linear system's impedance is sufficiently large. As a consequence, friction JND follows Weber's law, also when it is combined with mass–spring–damper dynamics, unless the level of friction approaches the detection threshold, which in turn can be influenced by the linear system dynamics. Based on the findings presented, it is possible to conduct targeted experiments to confirm and add to these initial results.**

***Index Terms*—Friction, haptics, human threshold, just-noticeable difference (JND), masking, mass–spring–damper system, perception.**

I. Introduction

In MANUAL control tasks where no direct link exists between the human control output (force) and the dynamic system being manipulated, haptic feedback becomes essential [1]. The benefits of this disconnect, however, are plentiful. Not only can haptic feedback be adjusted or extended to accommodate more intuitive control of complex dynamical systems, it is also possible to physically move the human controller to a different location, allowing for teleoperation [2], [3], [4]. In flight simulation, force-feedback combined with reliable models of aircraft control force dynamics is crucial to help pilots develop the proper muscle memory in training [5], [6], [7].

Manuscript received 25 July 2023; revised 22 November 2023; accepted 14 February 2024. Date of publication 22 March 2024; date of current version 17 May 2024. This article was recommended by Associate Editor X. Hu. *(Corresponding author: M. M. van Paassen.)*

This work involved human subjects or animals in its research. Approval of all ethical and experimental procedures and protocols was granted by Delft University of Technology Human Research Ethics Committee, decision Oct. 11, 2021, performed in line with WMA Declaration of Helsinki, 2013.

The authors are with the Control and Simulation section, Faculty of Aerospace Engineering, TU Delft, 2628 CD Delft, The Netherlands (e-mail: m.m.vanpaassen@tudelft.nl).

Color versions of one or more figures in this article are available at https://doi.org/10.1109/THMS.2024.3368358.

Digital Object Identifier 10.1109/THMS.2024.3368358

Due to inaccuracies in the force-feedback, resulting from limitations in control loading system (CLS) hardware and software as well as imperfect modeling of the control forces, haptic displays may never reach perfect transparency [8]. When applying a human-centric approach to haptic display design and considering the limited resolution of human perception, achieving *perfect* transparency becomes irrelevant.

Similar to perceiving changes in many other quantities, the thresholds for perceiving changes in haptic feedback follow the relationships for just-noticeable differences (JNDs) formulated by Weber [9]. In human-centric design, knowledge of these JNDs drive the required transparency of haptic displays, as it is unnecessary to aim for haptic display transparency beyond a level at which further improvement is imperceivable.

The Weber–Fechner law states that JNDs will be a fraction of the reference stimulus intensity [10]. Jones et al. [11], [12] showed that this law applies to force-feedback for dynamical systems when looking at system properties in isolation, studying the perception of stiffness and viscosity/damping. Rank et al. [13], among others, showed that in systems where these properties act simultaneously, as in mass–spring–damper systems, there is an interaction between them that may change the JNDs obtained in isolation. Since mass–spring–damper systems are common in manual control systems, these interactions are crucial when investigating force-feedback JNDs.

Fu et al. [14], [15], [16] studied this problem and formulated a unifying model for JNDs in linear system dynamics. This model extends Weber's law and, under the assumption that humans use a test input with a dominant frequency, states that the JNDs for stiffness, mass, or damping are proportional to the *magnitude* of the frequency response function (FRF) of the complete system dynamics, which can then be generalized to higher order systems [16]. But where the model of Fu et al. [17] only deals with linear systems, Coulomb friction is a nonlinear component relevant in many control tasks, particularly for the CLS of flight and helicopter simulators.

Gueorguiev et al. [18] studied the JND in friction, in isolation, and found constant Weber fractions for Coulomb friction. Messaoud et al. [19] confirmed these results. Because Coulomb friction is defined as a constant force opposing the direction of movement at nonzero velocity it can indeed be expected to follow the Weber–Fechner law. This research focused on tactile perception of touch displays, where friction accounts for most of the haptic feedback. Hence, the effects of friction JND in the presence of mass–spring–damper dynamics, as found in most control manipulators, need to be investigated.

This article builds upon Fu's unifying JND model [16] and extends it to the nonlinear case by adding friction. Two fundamental research questions must be addressed for this model extension: 1) *What is the friction JND in the presence of second-order system dynamics?* and 2) *How does friction, when added to a second-order system, affect the stiffness, mass, and damping JNDs?* The research presented here focuses on the first question and aims to identify all properties of the mass–spring–damper system that affect the friction JND. In addition, a first hypothesis is formulated of a model of friction JNDs in the presence of second-order dynamics.

The rest of this article is organized as follows. Section II discusses the theoretical background and provides initial analyses leading to an experiment in Section III. Experimental results are shown in Section IV and discussed in Section V. Finally, Section VI concludes this article.

II. Theoretical Background

A. JND for Second-Order Dynamics

Previous research dealt with JND masking effects within linear systems, most notably JND experiments performed by Fu et al. [16] and Caldiran et al. [20]. Both investigated the masking problem by studying it in the frequency domain. This means determining JNDs in the real or imaginary parts of the FRF of a given system [16], or JNDs in its magnitude and phase response [20].

Given a general second-order system $H(j\omega)$, with $\Delta\Re H(j\omega)_{\text{jnd}}$ and $\Delta\Im H(j\omega)_{\text{jnd}}$ as the JND in the real and imaginary parts of the system's FRF, respectively, the unified JND model formulated by Fu et al. is given by

$$\frac{\Delta\Re H(j\omega)_{\text{jnd}}}{|H(j\omega)|} \approx \frac{\Delta\Im H(j\omega)_{\text{jnd}}}{|H(j\omega)|} = \text{constant}. \tag{1}$$

Since the real part of the system FRF consists of the *in-phase* components of its impedance, $\Delta\Re H(j\omega)_{\text{jnd}}$ is the *coupled* JND in stiffness k and mass m

$$\Delta\Re H(j\omega)_{\text{jnd}} = \Delta k_{\text{jnd}} - \Delta m_{\text{jnd}} \cdot \omega^2. \tag{2}$$

The *out-of-phase*, imaginary part of the system's response $\Delta\Im H(j\omega)_{\text{jnd}}$ is the JND in damping b

$$\Delta\Im H(j\omega)_{\text{jnd}} = \Delta b_{\text{jnd}} \cdot \omega \cdot j. \tag{3}$$

Using Fu's model, the individual JNDs in stiffness, mass and damping can be expressed as a function of the system's initial stiffness, mass, damping as well as the excitation frequency ω. When drawing a system's response in the complex plane, this JND model states that a region can be defined, proportional in size to its magnitude response, inside which changes to the system fall within the JND and will not be perceived.

Caldiran et al. [20] conducted experiments where JNDs in firmness and bounciness were studied, which correspond to JNDs in the magnitude response of the second-order system or its phase response, respectively. Note that whereas Fu et al. used a side-stick, controlled by an electrohydraulic motor, for the haptic feedback, Caldiran et al. studied the JNDs for pressing a surface with a single finger using a Phantom Premium 1.0 device. They found that the JND in magnitude response of the system was independent of the phase, whereas the JND in the phase response increased monotonically.

Combining both investigations, it is possible to hypothesize on the actual shape of the region of no change in perception, when representing a mass–spring–damper system in the complex plane. While Fu argued that this region could be either elliptical or circular [16], for the practical application of a unified JND model for CLS design, this may be irrelevant.

Current requirements on CLS transparency as given by the European Union Aviation Safety Agency (EASA) [6] or the U.S.' Federal Aviation Administration (FAA) [7] are quite stringent and ignore human perception limits. Implementing even the most conservative model of human perception (using the lowest JNDs) would already be a considerable step in improving the match between device requirements and human perceptual capabilities, alleviating the CLS requirements.

B. Equivalent Linear Systems

Friction is an important aspect of haptic feedback in most CLS designs. Especially in aerospace manipulators, friction accounts for a significant part of the control forces [17]. Research on JNDs in friction is limited, however, and mostly considers friction on tactile displays [18], [19] [21], [22]. When considering the perception of friction while sliding a finger across a surface, mechanoreceptors in the skin dominate [22]. These results may not translate well to the perception of flight stick impedance. Research conducted by Gueorguiev et al. [18] (using a tactile display) found constant Weber fractions for JNDs in friction, consistent with earlier research into stiffness and damping JNDs [11], [12]. The research in this article, however, focuses on potential masking effects of stiffness, mass, and damping on the friction JND and no literature was found discussing this specific topic.

When modeling friction, several approaches exist. A most basic friction model is Coulomb friction, where friction is described as a constant force opposing the direction of movement [23]. More elaborate commonly used friction models include the Dahl model [24] and the LuGre model [25], where Dahl's model of friction deals with the break-away effect, describing the presliding haptic feedback, the LuGre model adds viscous friction and the Stribeck effect, which describes the transition from static friction to dynamic friction. Even though CLSs commonly incorporate static friction [17], for the purpose of this research it was decided to focus on dynamic friction only. As stated before, no research has been done yet on the specific research question introduced in this article. It was therefore decided to first investigate JNDs using a model considering dynamic Coulomb friction before introducing the less significant (in terms of perceived forces) nonlinear effects present in the Dahl's model and the LuGre model.

Considering Coulomb friction, for a mass–spring–damper system with friction added, the system dynamics are

$$m\ddot{x}(t) + b\dot{x}(t) + f\,\text{sgn}(\dot{x}(t)) + kx(t) = F(t) \tag{4}$$

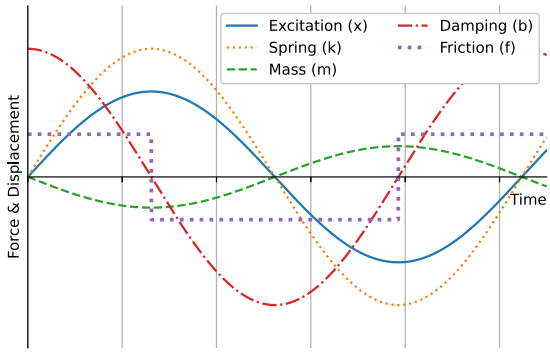

Fig. 1. Individual contributions from mass–spring–damper parameters, as well as friction, to the system's impedance when harmonically excited.

where $F(t)$ represents the force (or torque) resulting from a displacement $x(t)$, f is the friction coefficient, and $\mathrm{sgn}()$ is the signum function. When considering a harmonic excitation of this system, the contributions of the spring, mass, damper, and friction (exaggerated friction for clarity) to the impedance are illustrated in Fig. 1. The analysis is performed by calculating the force $F(t)$ (impedance) as a result of the excitation $x(t)$ because the control tasks considered in this article are displacement (excitation) tracking tasks. It should be noted that this figure holds for any sinusoidal motion so force ($F(t)$) could easily be replaced by torque ($T(t)$), in which case the excitation would be an angle and the mass would be represented by the moment of inertia.

Similar to the damping contribution, friction forces act out-of-phase to the harmonic excitation. When all individual contributions in Fig. 1 are added, Fig. 2(a) can be constructed. The nonlinear system response including friction will in the following be approximated linearly in two different ways: the maximum impedance model and the phase-shift model.

1) Maximum Impedance Model: When considering the system's total impedance to a harmonic excitation, one approach of approximating the system with friction linearly would be to increase the magnitude response of the linear system while keeping its phase response constant. The equivalent linear dynamics can then be described as follows:

$$|H(j\omega)|_{\text{eq}} = |H(j\omega)| + f, \quad \angle H(j\omega)_{\text{eq}} = \angle H(j\omega) \tag{5}$$

where $H(j\omega)$ represents the original mass–spring–damper system and f the friction force (or torque when considering rotational stick motion).

The response of the maximum impedance model is illustrated in Fig. 2(a). Clearly, where this approach does not take into account the instantaneous changes in force occurring at the extremes of the excitation, it does deal with the increased amplitude of the impedance signal.

2) Phase-Shift Model: The maximum impedance model approximates the nonlinear system with friction quite well at the extremes of the impedance, but not for the regions in between. Here, the system with friction can be best approximated by introducing a phase-lead to the linear frictionless system, which makes sense from the earlier realization that friction, such as

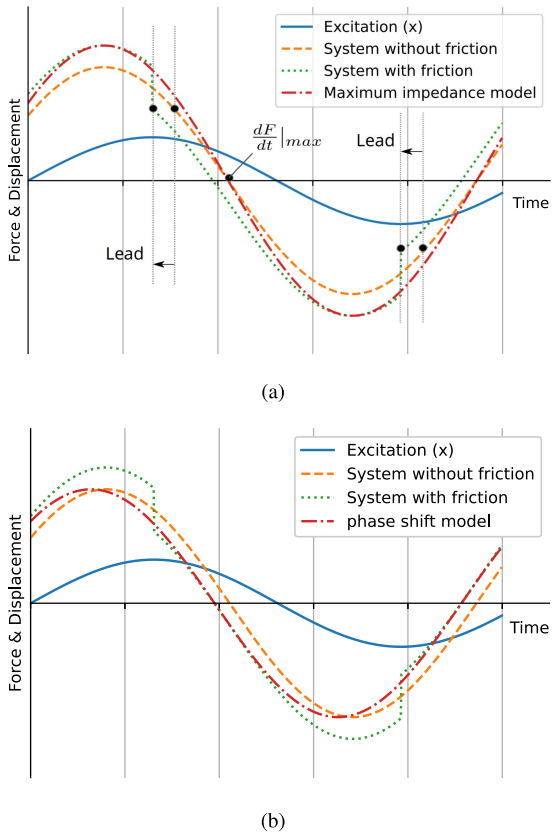

Fig. 2. Impedance of mass–spring–damper system with and without friction, illustrating equivalent linear dynamics using the maximum impedance model (a) and using the phase shift model (b). Note that since $\angle H(j\omega) < \pi/2$ a phase-*lead* is applied, see text. (a) Maximum impedance model. (b) Phase shift model.

damping, acts out of phase. This phase shift, as caused by friction and visualized as a phase lead in Fig. 2(a), can be determined by shifting the original linear system over the x-axis until it intercepts the system with friction at the crossing of the x-axis. Defining the excitation (displacement) $x(t)$ as $x(t) = \sin(\omega t)$, the impedance $F(t)$ follows from the magnitude and phase response of the second-order system:

$$F(t) = |H(j\omega)| \sin(\omega t + \angle H(j\omega)). \tag{6}$$

The time-derivative of force, dF/dt is then given by

$$dF/dt = |H(j\omega)| \cdot \omega \cdot \cos(\omega t + \angle H(j\omega)). \tag{7}$$

At the moment of crossing the x-axis, dF/dt is at its maximum, where dF/dt at the x-axis crossings is defined as

$$dF/dt|_{\text{max}} = |H(j\omega)| \cdot \omega. \tag{8}$$

The difference in force between both systems, with or without friction, at any given time will be due to the friction force f. The shift in time, t_{shift} is then given by

$$t_{\text{shift}} = f \cdot \frac{dt}{dF} = \frac{f}{|H(j\omega)| \cdot \omega} \tag{9}$$

with corresponding phase shift ϕ_{shift}

$$\phi_{\text{shift}} = \omega \cdot t_{\text{shift}} = f/|H(j\omega)|. \tag{10}$$

Fig. 2(b) shows the equivalent linear dynamics, with the phase lead in place. The approximation matches the nonlinear system with friction only in the regions between maximum impedance.

The phase-lead from this equivalent dynamics phase-shift model becomes a phase-*lag* when the linear system's response $\angle H(j\omega)$ has a phase $\phi > \pi/2$ rad. However, in real-world applications (and excitation frequencies) the control force dynamics phase response will practically always fall within the bounds of $0 < \phi < \pi/2$, as will also be assumed here.

C. Applying Equivalent Linear System Models

Given the equivalent linear dynamics models, it is now possible to apply Fu's theory and hypothesize about the role of second-order dynamics on friction JNDs. Where Fu described the JND in the real and imaginary parts of a second-order system's FRF, changes in the real and imaginary part of a system can also be described by a simultaneous change in magnitude response and phase. In the perception of dynamic systems, both motion x and force F cues are important. Together, these cues can be combined to distinguish between different springs or dampers. Fu et al. [26] performed an experiment where the relationship between these two cues was studied by performing JND measurements of spring stiffness. They found that when controlling for force—by having subjects apply the same force on different springs resulting in different displacements—JNDs in spring stiffness were higher when compared to controlling for displacement (where the displacement was constant and the different force was the main cue). This experiment showed that without visual feedback, the displacement can be difficult to use as a cue for discriminating stiffnesses.

From these findings, it is possible to hypothesize that the increased *magnitude*, as caused by adding friction to a linear system, is of more importance than the apparent phase changes in discriminating levels of friction when no visual feedback is available. However, when there is a clear visual displacement cue, which is necessary for analyzing JNDs in the frequency domain (requiring a constant harmonic excitation which can be induced by a preview tracking task), a changed phase response may equally contribute. In addition, when discussing the region of no noticeable difference, expressed around the FRF in the complex plane (illustrated in Fig. 3), Fu hypothesized [16] it could be circular, which would imply a great sensitivity also for a change purely in the phase response.

Taking this into consideration, both approaches of equivalent linear dynamics (maximum impedance model and phase-shift model) could be relevant in exploring JNDs in friction from the perspective of Fu's JND model. For a second-order system with a phase response $0 < \phi < \pi/2$ the time domain response of the equivalent linear dynamics system combining both models is plotted in Fig. 4, as well as both models' frequency responses in the complex plane in Fig. 3. The visualization in the time domain follows from a system alternating between an increased magnitude response and a phase-lead at four times the excitation frequency. What is most important to recognize is that for the systems discussed, the two alternating models approach the nonlinear system reasonably well. Therefore, both linear approximation models could play a role in the perception of friction, including the threshold, and Fu's JND model can be applied to both models.

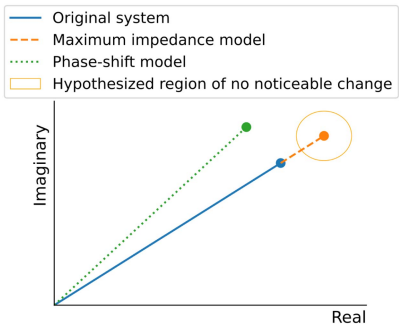

Fig. 3. Complex plane representation of equivalent linear dynamics, showing both maximum impedance and phase-shift models while indicating the region of no noticeable change according to Fu et al. [16].

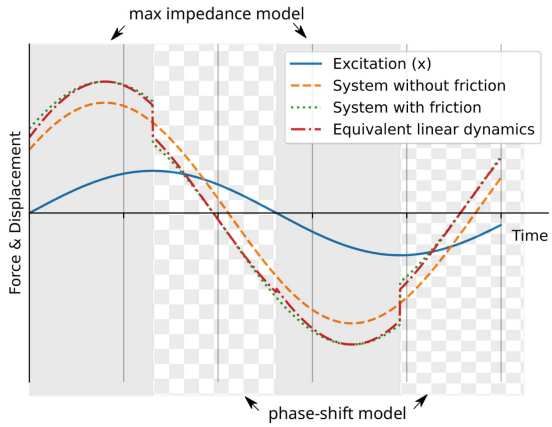

Fig. 4. Visualization of impedance of mass–spring–damper system including and excluding friction, illustrating the combined equivalent linear dynamics by alternating the maximum impedance model and phase-shift model.

D. Perception of the Nonlinear Force Change

The attempt to find equivalent linear dynamics does not deal with an important part of the perceived forces due to friction, which is the nonlinear force change itself, occurring at the moment of direction change. This sudden change in force, or *force-drop*, cannot be described using second-order dynamics. Nonetheless, this drop may be, consciously or subconsciously, perceived and compared when distinguishing different levels of friction. Weber's law defines the threshold for perceiving changes in force, the JND, as the constant portion of the reference force from which the change occurs [9]. This law holds over a wide range of sensory modalities and only breaks down in regions where the stimulus intensity is close to the detection threshold [27]. The JND is then no longer a constant portion of the reference stimulus intensity but increases.

A possible hypothesis for friction JNDs in the presence of second-order dynamics is that the force-drop is used for the perception of friction independently of other dynamics. For friction when perceived in isolation, the little available research

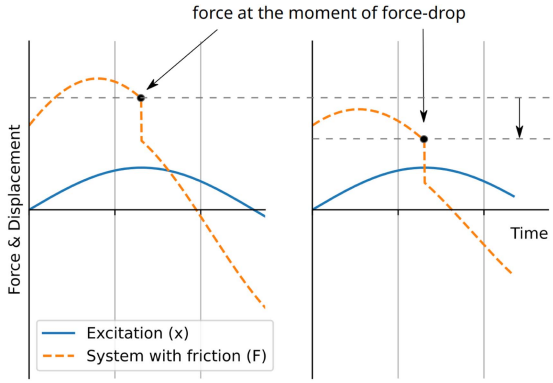

Fig. 5. Effect of lowering $\Re H(j\omega)$ on the force at the moment of the force-drop caused by friction.

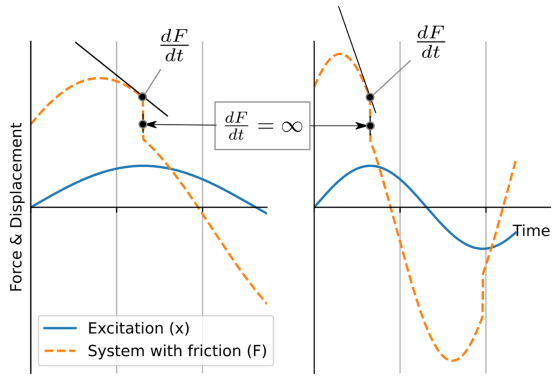

Fig. 6. Effect of increasing the excitation frequency ω on the dF/dt at the moment of the force-drop caused by friction.

shows Weber's law to hold [18], [21]. This may not be surprising since the perception of (Coulomb) friction in isolation, when perceived in motion, should be very similar to statically perceiving a constant force like the original weightlifting experiments performed by Weber himself [10]. However, when other forces due to interactions with mass–spring–damper dynamics are present, this friction force may be more difficult to distinguish. Nevertheless, the force-drop itself could still be used in the perception and even the perception of differences (or JNDs). If this force-drop *is* perceived, as a stimulus above some detection threshold, then it is possible that a mass–spring–damper system has no influence on the friction JND and it is only proportional to reference friction. In other words, *the change in force-drop that is just perceivable is then a constant fraction of the reference force-drop.*

The main properties that are expected to affect the force-drop perception are the real part of the second-order system $\Re H(j\omega)$ (determined by the second-order system mass m and stiffness k), its phase $\angle H(j\omega)$ and the excitation frequency ω. The real part $\Re H(j\omega)$ is responsible for the force occurring at the extremes of the excitation; here, velocity is zero and damping plays no role. If the perception of the force-drop itself follows Weber's law, then for an equal change in force, the force from which this change occurs (the reference force) determines whether the change is perceived. In other words, when $\Re H(j\omega)$ is relatively large, the instantaneous force change occurring at the extremes of the excitation may be less likely to be perceived compared to a smaller $\Re H(j\omega)$. This effect is illustrated in Fig. 5.

Decreasing $\Re H(j\omega)$ also causes a shift of the phase at which the force-drop occurs. Since the force-drop can be described as an infinite derivative of force with respect to time dF/dt, when this drop in force coincides with a large value for dF/dt of the system's impedance, there could be a masking effect that is not present at lower dF/dt levels. Reasoning in a similar way then explains the potential effect of the excitation frequency ω on perceiving the force-drop, as both frequency and phase can affect the value of dF/dt at the moment of the force-drop. Fig. 6 illustrates how ω potentially masks the force-drop by scaling dF/dt, see (7). The $\angle H(j\omega)$ determines the phase at which the force-drop occurs and therefore potentially indirectly affects dF/dt.

III. Experiment

A. Hypotheses

Based on Section II, a number of hypotheses can be stated on the JND in friction when presented together with mass–spring–damper dynamics. In this first investigation, we stated three hypotheses.

The first and simplest hypothesis would be that no masking effect of the second-order system on friction exists.

H.1 *Friction JND is proportional to the reference friction setting, independent of mass–spring–damper parameters.*

This would be the case if the friction is perceived independently of other dynamics, most likely when nonlinear force changes dominate its perception. The friction JNDs are then expected to be constant fractions of the reference friction, satisfying Weber's law, as previous research into friction JNDs without potential masking dynamics indicated [18], [21]. The first hypothesis can be mathematically expressed as

$$\frac{\Delta f_{\text{jnd}}}{f} = \text{constant} \tag{11}$$

with f the reference friction level.

The second hypothesis follows from the possibility that some form of masking occurs due to the mass–spring–damper system. The analysis of linear equivalent dynamics can be applied to Fu's JND model to construct the second hypothesis. Using the description of equivalent dynamics, both the maximum impedance and phase-shift models of equivalent dynamics result in a hypothesis of the friction detection threshold, as well as the JND. For friction to be detected, Fig. 3 illustrated that the Euclidean distance between the two different models of equivalent dynamics in the complex plane should be larger than the region of no noticeable change. Then, considering the JND, for a difference in friction to become noticeable, it needs to fall outside of the detection threshold of the equivalent dynamics system including friction, meaning the JND in friction would be close to the detection threshold, with the latter depending on the second-order system settings. The second hypothesis can then be formulated as follows.

TABLE I
EXPERIMENT MANIPULATION AND CONDITIONS (REPEATING CONDITION 2, SEE TEXT)

Manipulation and conditions		$\lvert H(j\omega)\rvert$	$\angle H(j\omega)$ [rad]	$\Re H(j\omega)$	$\Im H(j\omega)$	k [Nm/rad]	m [kgm^2]	b [Nms/rad]	ω [rad/s]	f [Nm]	$f/\lvert H(j\omega)\rvert$ [Nm]
	1	2.12	0.79	1.5	1.5	1.87	0.01	0.25	6	**0.1**	0.047
f	**2**	2.12	0.79	1.5	1.5	1.87	0.01	0.25	6	**0.15**	0.071
	3	2.12	0.79	1.5	1.5	1.87	0.01	0.25	6	**0.2**	0.094
	4	**1.6**	0.79	1.13	1.13	1.49	0.01	0.19	6	0.15	0.093
$\lvert H\rvert$	**2**	**2.12**	0.79	1.5	1.5	1.87	0.01	0.25	6	0.15	0.071
	5	**2.6**	0.79	1.84	1.84	2.2	0.01	0.31	6	0.15	0.058
	6	2.12	**1.02**	1.10	1.81	1.74	0.01	0.23	**8**	0.15	0.071
$\angle H, \omega$	**2**	2.12	**0.79**	1.5	1.5	1.87	0.01	0.25	**6**	0.15	0.071
	7	2.12	**0.40**	1.95	0.83	2.04	0.01	0.28	**3**	0.15	0.071
	8	2.12	**1.02**	1.10	1.81	1.46	0.01	0.3	6	0.15	0.071
$\angle H$	**2**	2.12	**0.79**	1.5	1.5	1.87	0.01	0.25	6	0.15	0.071
	9	2.12	**0.40**	1.95	0.83	2.31	0.01	0.14	6	0.15	0.071

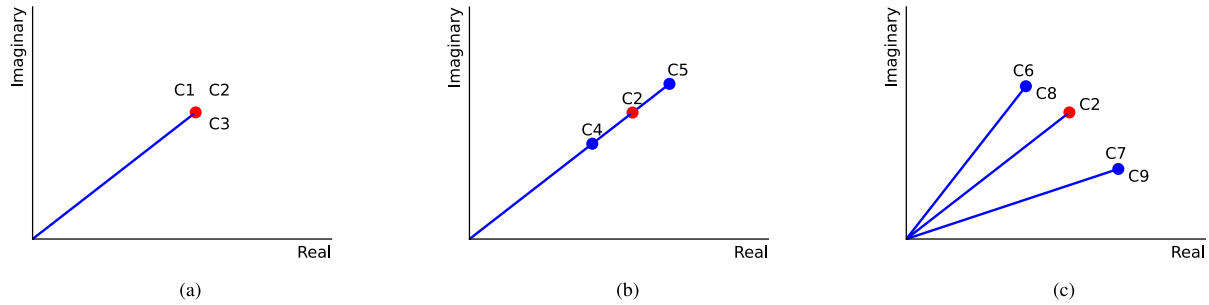

Fig. 7. Visualization of the four sets of three conditions. Conditions 6 and 8 as well as 7 and 9 differ only in excitation frequency ω, see Table I. (a) First set (1, 2, 3): constant $H(j\omega)$ and varying reference friction f. (b) Second set (4, 2, 5): varying $|H(j\omega)|$ and constant reference friction f. (c) Third (6, 2, 7) and fourth (8, 2, 9) sets: varying $\angle H(j\omega)$ with a constant and varying excitation frequency ω, respectively.

H.2 *The friction JND follows from Fu's JND model, where JNDs in friction are proportional to the magnitude response of the equivalent linear system.*

The second hypothesis can be mathematically expressed as

$$\frac{\Delta f_{\text{jnd}}}{|H(j\omega)|_{\text{eq}}} = \text{constant}. \tag{12}$$

The third hypothesis stems from the discussion in Section II-D, where it was suggested that the instantaneous force-drop in the system response could play a key role in the perception of friction and changes in friction. Potential factors masking the perception of this force-drop are $\Re H(j\omega)$, $\angle H(j\omega)$ as well as the excitation frequency ω. Because $\angle H(j\omega)$ and $\Re H(j\omega)$ are *coupled*, and for a constant magnitude response cannot be considered in isolation, the third and final hypothesis is as follows.

H.3 *The friction JND is influenced by second-order system excitation frequency* or *system phase response independently of its magnitude response.*

B. Experiment Conditions

The effects of mass–spring–damper dynamics on friction JND will be investigated. JNDs will be determined for several conditions of second-order system parameters and reference friction settings. From the hypotheses given in Section III-A, *four* parameters can be identified that could independently affect the JND in friction. These are:

1) the level of friction (the reference friction setting f);
2) the magnitude response of the second-order system $|H(j\omega)|$;
3) the phase-response $\angle H(j\omega)$; and
4) the excitation frequency ω.

A full factorial design of manipulating these four independent variables would result in a large experiment matrix, requiring a high number of participants. In this experiment, a different approach is taken. Four sets of three conditions will be used to test each of their influences on the JND in friction independently. Condition 2 will act as the "baseline" condition and repeated in all four sets. Table I illustrates that then nine conditions are needed to make up four sets of three, all comparing a change of f, $|H(j\omega)|$, $\angle H(j\omega)$, or ω with Condition 2. An overview of all condition settings is given by Table I and visualized by Fig. 7.

To test Hypothesis H.1 (the perception of friction follows Weber's law independent of system dynamics) a first set of three conditions (1, 2, 3) is defined where the reference friction f is varied, while keeping the system dynamics $H(j\omega)$ constant, Fig. 7(a), Table I. By varying the friction, it is possible to determine whether Weber's law holds for friction JNDs when constant mass–spring–damper dynamics are present. Furthermore, for Hypothesis H.1 to hold, changing $|H(j\omega)|$, $\angle H(j\omega)$, and ω, as will be done in the following, should *also* have no significant effect on JNDs in friction.

To test Hypothesis H.2, the friction JND is determined for different magnitude responses of the potentially masking mass–spring–damper system $|H(j\omega)|$, while keeping the reference friction f constant. Whether friction JND is indeed proportional to the magnitude response of the equivalent linear system

dynamics $|H(j\omega)_{\text{eq}}|$ will be tested with this second set of three conditions (4, 2, 5), Fig. 7(b), Table I.

Finally, Hypothesis H.3 considers the possibility that the second-order system's phase response or excitation frequency affects the friction JND. If this is indeed the case, varying both parameters while keeping the reference friction f and $|H(j\omega)|$ constant should show an effect on friction JNDs. Therefore, in the final two sets of conditions, three different second-order system phase responses $\angle H(j\omega)$ will be considered, Fig. 7(c), Table I. In one series of three settings, $\angle H(j\omega)$ is adjusted by changing $\Re H(j\omega)$ and $\Im H(j\omega)$ while keeping $|H(j\omega)|$ constant (Conditions 8, 2, 9). In the other series, the excitation frequency ω is varied (Conditions 6, 2, 7) with $\Re H(j\omega)$ and $\Im H(j\omega)$ adjusted in such a way as to keep the phase and magnitude response of $H(j\omega)$ the same in both sets of conditions. Both series are illustrated in Fig. 7(c).

With Conditions 6 and 8, as well as 7 and 9, being matched in phase response, differences in friction JND due to excitation frequency not accounted for by phase differences can be studied. That is, when $\angle H(j\omega)$ affects the friction JND but the excitation frequency does not, then no difference should be found between Conditions 6 and 8 or 7 and 9. If, however, excitation frequency affects friction JND independently of $\angle H(j\omega)$, JNDs for Condition 6 should differ from Condition 8 as should the JNDs for Condition 7 from 9.

C. Apparatus and Participants

The experiment was performed at the Human–Machine Interaction Laboratory at Aerospace Engineering (TU Delft), Fig. 8(a). The admittance controlled side-stick (right hand) manipulator presents the haptic feedback to participants and is driven by an electrohydraulic motor (bandwidth $\approx$ 40 Hz). A simulation program, running at 2500 Hz, controlled the side stick, simulating the dynamics of a mass, spring, and damper device with friction. All parameters (mass, spring, damping, friction) could be adjusted on-line. In a trial, the friction level of the comparison conditions was adjusted for each comparison, according to the fraction indicated by the staircase procedure. All visual cues were displayed on an 18 inch LCD screen 80 cm in front of the subjects. The side-stick was limited to move only laterally (rotate left and right).

The experiment was approved by the TU Delft Human Research Ethics Committee (ID:1827) and involved nine participants (eight males, one female). At the time of the experiment, TU Delft COVID protocols only allowed for inviting the minimum number of subjects. Participants had no impairment of the right arm and showed during a 20-min training, preceding the measurements, their ability to perform the experiment tasks.

D. Experiment Setup and Procedure

For each participant, the friction JND was determined for all nine conditions through an adaptive one-up/two-down staircase procedure [14], selecting one-up/one-down until the first reversal to realize faster convergence. The stepwise downwards/upwards ratio was set at 0.5488, converging to a JND with an 80.35% correct performance [28]. The staircase finished after the seventh reversal (change in direction of the staircase) or when reaching 40 trials. The last four reversals were averaged to calculate the JNDs. To balance effects of learning and fatigue, a Latin square design was chosen.

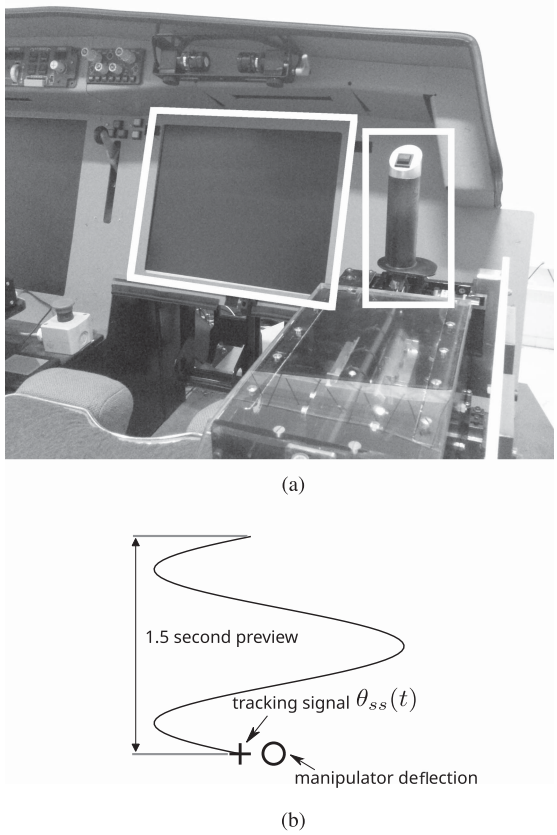

Fig. 8. Experimental devices (the side-stick manipulator and LCD screen), and the preview tracking task. (a) Experimental setup. (b) Tracking task.

In terms of haptics, in each step, subjects were presented with a reference level of friction, fixed within each experiment condition and indicated in Table I, as well as a comparatively higher level of friction, investigating the *upper* JNDs only. Then a two-alternative forced-choice method was used, where the subject indicated for which of the two trials the side-stick was perceived as having a "higher resistance to movement," resulting in answers either correct or false, leading to stepping up or down in the staircase procedure.

Similar to the experiments performed by Fu et al. [14], each step of the staircase presented the participant with two 6.3 s segments of a preview tracking task, Fig. 8(b), with a tracking signal described by $\theta_{ss}(t) = 0.37 \cdot \sin(\omega t)$, with θ_{ss} being the commanded stick deflection angle in radians and ω the excitation frequency. The visual display also showed a progress bar at the top, indicating which of the two trials was running. To accommodate a smooth transition, going from no movement to the ω rad/s excitation, the first and last seconds of the 6.3 s segments were used as a fade-in and fade-out phase, respectively. During these fade-in/fade-out phases, the amplitude of the sinusoidal displacement function was linearly interpolated (in time) between 0 and 0.37.

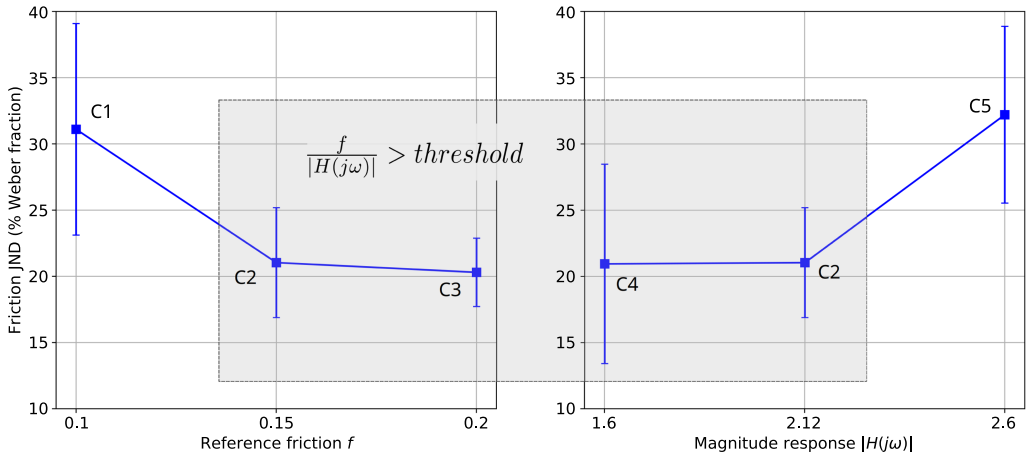

Fig. 9. Results of the first two sets of three experiment conditions [corresponding to Fig. 7(a) and (b)], showing means and 95% confidence intervals for friction JND Weber fractions, with on the left-hand plot an increasing reference friction f for a constant $H(j\omega)$ (Conditions 1, 2, 3), and on the right-hand plot an increasing $|H(j\omega)|$ for a constant reference friction f (Conditions 4, 2, 5). Data for the baseline Condition 2 are repeated in this figure.

Participants were instructed and briefly trained to concentrate on following the tracking signal while still focusing part of their attention on perceiving the side-stick resistance. The experimenter would check, on a separate screen, whether the tracking task was followed with desirable accuracy and would give feedback on this performance if necessary.

E. Statistical Analysis

The measurement data are in the form of friction levels at moments of reversal for every participant and every condition. With nine participants and nine conditions, the 81 JNDs are calculated by averaging the friction levels of the last four out of seven reversals. The 9×9 matrix was normalized to both reference friction and equivalent dynamics to establish Weber fractions. After checking for sphericity using Mauchly's test, a one-way repeated-measures analysis of variance (ANOVA) is performed for each of the four independent variables introduced in Section III-B. With each variable progressively varying in three conditions, the significance of potential masking effects of the second-order system's magnitude response $|H(j\omega)|$, its phase-response $\angle H(j\omega)$, the excitation frequency ω, as well as effects of the reference friction f on friction JND, can be established independently. Significant results for the ANOVA ($p < 0.05$) will be followed-up by Tukey's honest significant difference (HSD) *post hoc* test to further explore the differences between groups. Furthermore, to distinguish the effect of phase-response $\angle H(j\omega)$ and excitation frequency ω on friction JNDs, paired samples t-tests will be performed.

IV. Results

When considering the results of the first and second set of three conditions, with reference friction and the magnitude response of the second-order system $|H(j\omega)|$, respectively, as the independent variables, [visualized in Fig. 7(a) and (b)], Fig. 9 shows the means and 95% confidence intervals for the JNDs in friction. The JNDs are normalized to reference friction presenting Weber fractions on the vertical axis (in percentages) and the independent variable settings (corresponding to Table I) are given on the horizontal axis. The plot on the left of Fig. 9 shows the JNDs for a varying reference friction and a constant $H(j\omega)$ (Conditions 1, 2, 3) and the plot on the right shows the JNDs for a constant reference friction and a varying $|H(j\omega)|$ (Conditions 4, 2, 5).

Fig. 9 shows that the Weber fractions are affected while changing the reference friction setting (left-hand plot) as well as from increasing the mass–spring–damper system magnitude response $|H(j\omega)|$ (right-hand plot). Both effects are indeed significant. The effect of reference friction with Conditions 1, 2 and 3: $F(2, 16) = 3.54$, $p = 0.04$, as well as the effect of $|H(j\omega)|$ with Conditions 4, 2, and 5: $F(2, 16) = 5.47$, $p = 0.01$. Furthermore, Tukey's HSD *post hoc* test demonstrates a significant difference (with p-values corrected for multiple comparisons) between Conditions 4 and 5 ($p = 0.02$) as well as Conditions 2 and 5 ($p = 0.02$) but not for Condition 1 and 2 ($p = 0.09$) or Condition 1 and 3 ($p = 0.06$). Comparing Conditions 2 and 3 and Conditions 2 and 4 where $\frac{f}{|H(j\omega)|}$ is relatively large indicates minimal differences ($p = 0.9$ for both comparisons).

Considering the three hypotheses stated in Section III-A it is clear that friction JND depends on mass–spring–damper dynamics, and Hypothesis H.1 is rejected. Friction JND *is* affected by the second-order system's magnitude response, as demonstrated by the results from Conditions 4, 2, and 5. In addition, for a constant second-order system, friction also does not seem to follow Weber's law, Conditions 1 to 3.

The second hypothesis stated that friction JND is proportional to the magnitude response of the equivalent linear system. From Fig. 9 it seems that the effects of both reference friction and $|H(j\omega)|$ setting on friction JND are not linear, while these parameters do vary linearly among Conditions 1 to 3 and from Conditions 4, 2 to 5, respectively. However, when normalizing friction JNDs to $|H(j\omega)_{eq}|$ and then testing the second hypothesis given by (12) on the first two sets of conditions, there are no statistically significant differences (Conditions 1,

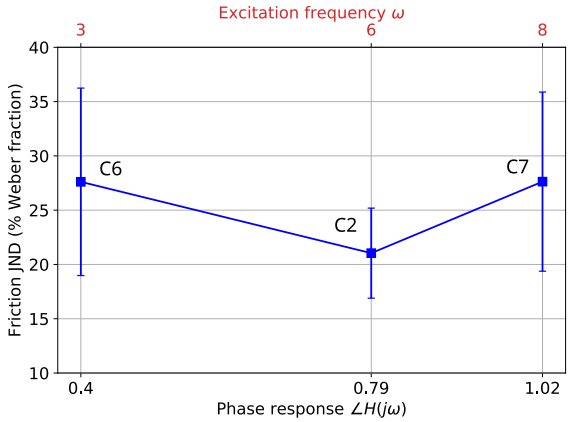

Fig. 10. Means and 95% confidence intervals of friction JND Weber fractions for Conditions 6, 2, and 7 with excitation frequency ω and $\angle H(j\omega)$ varying.

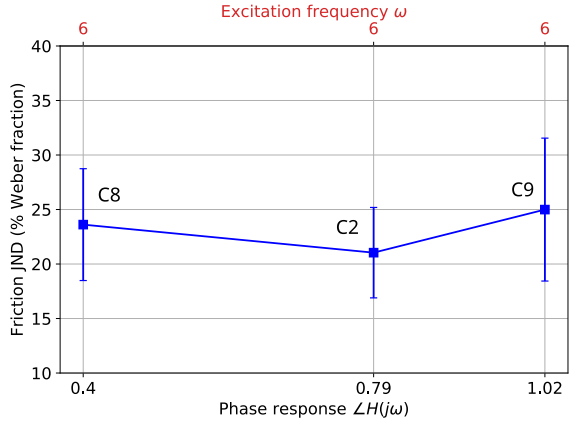

Fig. 11. Means and 95% confidence intervals of friction JND Weber fractions for Conditions 8, 2, and 9 with constant ω and $\angle H(j\omega)$ varying.

2, and 3: $F(2, 16) = 1.39$, $p = 0.27$; Conditions 4, 2, and 5: $F(2, 16) = 1.24$, $p = 0.31$). Therefore, Hypothesis H.2 cannot be rejected. However, simply accepting H.2 based on this test alone is precipitous. The apparent nonlinear change in friction JND as a result of varying $|H(j\omega)|$, visible in Fig. 9 and signified by Tukey's *post hoc* test, contradicts Hypothesis H.2 and indicates that the limited sample size could lead to a Type II error when H.2 is accepted.

For Conditions 2, 3, and 4, indicated by the gray area in Fig. 9, the Weber fractions are fairly constant [ANOVA: $F(2, 16) = 0.0262$, $p = 0.91$, Greenhouse–Geisser corrected p-value]. In fact, when considering the results from only these conditions, the first hypothesis does seem to hold with JNDs in friction following Weber's law (Weber fractions of around 20%). However, higher thresholds are found for Conditions 1 and 5, for which the friction component is small, in proportion to the mass–spring–damper system magnitude response $|H(j\omega)|$. See Fig. 7(a) and (b), and the calculation of $f/|H(j\omega)|$ in Table I. Keeping in mind the results from Tukey's *post hoc* test, demonstrating a lack of significant difference between Condition 2 and 4 or Condition 2 and 3, it is posited that for the conditions with a constant phase response (here $\pi/4$ rad), the Weber fractions for friction JND will indeed be constant, as long as the proportion of impedance magnitude accounted for by friction is large enough

$$f/|H(j\omega)| > \text{threshold}. \tag{13}$$

Tukey's *post hoc* tests applied to Conditions 4, 2, and 5, with $|H(j\omega)|$ as the independent variable, agrees with this finding: significant differences between Conditions 5 and 4/2, no significant differences between Conditions 2 and 4 (see Fig. 9). However, while the *post hoc* analysis of Conditions 1, 2, and 3, with reference friction as independent variable, shows a similar trend with minimal differences between Conditions 2 and 3, the differences between Conditions 1 and 2/3 are not significant.

The friction JND results for the third and fourth sets of conditions [see Fig. 7(c)], are plotted in Figs. 10 and 11, showing effects of excitation frequency ω and second-order system phase response $\angle H(j\omega)$ on friction JND, respectively. No significant differences are found as a consequence of varying phase response and excitation frequency [see Fig. 10] [ANOVA: $F(2, 16) = 0.78$, $p = 0.48$] or only varying phase response [see Fig. 11] [ANOVA: $F(2, 16) = 0.52$, $p = 0.61$].

It was explained in Section III-B that Conditions 6 and 8, as well as Conditions 7 and 9, can be compared to distinguish between the effects of excitation frequency ω and phase response $\angle H(j\omega)$. Whether ω affects the friction JND independently of $\angle H(j\omega)$ is something that cannot be inferred from these results, as the variances are simply too large to draw conclusions on the differences in means between Conditions 6 and 8 as well as 7 and 9. Paired samples t-tests demonstrate this lack of statistical significance, when comparing Condition 6 ($M = 27.6$, $SD = 13.2$) and Condition 8 ($M = 23.6$, $SD = 7.9$); $t(16) = 0.97$, $p = 0.36$, as well as Condition 7 ($M = 27.6$, $SD = 12.6$) and 9 ($M = 25.0$, $SD = 10.0$); $t(16) = 0.48$, $p = 0.65$.

V. Discussion

Experiment results show that the first hypothesis (friction JNDs follow Weber's law regardless of mass–spring–damper system setting), seems to hold for some conditions (2, 3, and 4, see Fig. 9). Nevertheless, Conditions 1 and 5 show a significant effect of both reference friction and second-order system magnitude response $|H(j\omega)|$ on friction JND, respectively. These increased Weber fractions could be caused by friction levels being closer to the detection threshold.

Weber's law has been shown to break down at the limits of perception (see Section II and also Norwich [27]). In our experiment, these limits could have been affected by the mass–spring–damper dynamics. That is, the second-order system dynamics do not *directly* affect the friction JND, but *do* influence the detection threshold for friction, and by raising that detection threshold the Weber fractions for friction JNDs will increase. This will be explained using Fig. 12.

When regarding the results of Figs. 9 and 12 illustrates how varying the reference friction in the presence of fixed second-order system dynamics (Conditions 1, 2, and 3) leads to an asymptotic increase in Weber fractions for friction JND. Also, considering Conditions 4, 2, and 5, it can be observed

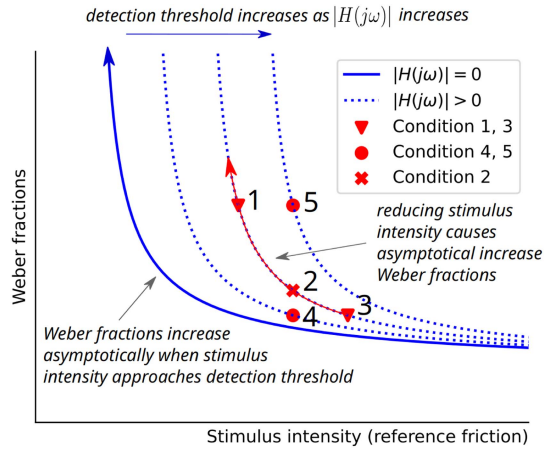

Fig. 12. Sketch of the asymptotic increase in Weber fractions of friction JND as a result of changing the reference friction (Conditions 1, 2, and 3) or an increasing detection threshold as $|H(j\omega)|$ gets larger (Conditions 4, 2, and 5). Both changing the reference friction, as well as increasing the detection threshold, show similar effects on the friction JND Weber fractions.

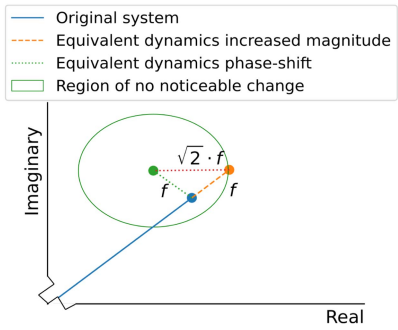

Fig. 13. Illustrating the instantaneous change in system dynamics on the complex plane with the region of no noticeable change derived from Fu's JND model. This example shows (zoomed in) experiment Condition 2.

that varying $|H(j\omega)|$ while keeping reference friction constant causes the *same* asymptotic increase in Weber fractions.

In Section II-B, using the equivalent linear dynamics theory, some suggestions have been made as to what the detection threshold depends on. It was hypothesized that either a change in equivalent linear dynamics magnitude or phase response, or a perception of the nonlinear force-drop, would determine whether friction is perceived or not. These hypotheses focused on friction JND rather than the detection threshold for friction.

The same theory can nevertheless be applied to argue the validity of the suggestion expressed before (and visualized in Fig. 12) that the second-order system's magnitude response affects the friction detection threshold. Considering the levels of friction tested, it seems that the equivalent linear system dynamics increased magnitude and phase response cannot explain its perception fully., e.g., a friction level of 0.15 Nm is most likely well above the detection threshold in a system where $|H(j\omega)| = 2.12$ (from its JND Weber fraction in Conditions 2, 3, and 4 from Fig. 9). However, applying Fu's JND model [16], the resulting equivalent magnitude and phase response changes from friction fall well within the detection threshold established by Fu

$$f/|H(j\omega)| = 0.15/2.12 = 0.07 \tag{14}$$

where Fu found Weber fractions of around 10%, the increased magnitude response due to friction leads to values around 7%. Then again, it is possible that the nonlinear force-drop occurring at a change in excitation direction is responsible for the perception of friction *before* the change in magnitude response plays any role. Where Fu had participants experience different mass–spring–damper system settings with a small break in-between trials, friction can be described by a sudden shift in system parameters *within* the trial. This difference could cause the Weber fractions to be lower, even while still depending on $|H(j\omega)|$.

Furthermore, when looking at the instantaneous change in equivalent linear system dynamics within a sinusoidal excitation, while applying Fu's JND model, it can be seen that this instantaneous change is actually larger than the level of friction. This is considering that the system including friction is best described in linear terms by a system "alternating" between the earlier described maximum impedance model and the phase-shift model (see Fig. 3). It was derived in (10) that the phase shift describing the instantaneous drop in force because of introducing friction is given by $f/|H(j\omega)|$. Using the small-angle approximation, it is found that the Euclidean distance, in the complex plane, from the original frictionless system to the maximum impedance model system [which is the level of friction f as (5) indicates] is equal to the distance from the original system to the phase-shift model system, as illustrated in Fig. 13. Considering the angle between the original system and the phase-shift or maximum impedance model is approximately equal to 90°, the perceived instantaneous change in $\Re H(j\omega)$ due to friction is then described by $\sqrt{2} \cdot f$, see Fig. 13.

Now from these realizations and Fig. 13, together with the recognition that the size of the region of no noticeable change depends on $|H(j\omega)|$, which follows from Fu's JND model, a possible explanation is presented for $|H(j\omega)|$ affecting the detection threshold for friction. The hypothesis is that if the instantaneous shift in perceived dynamics caused by friction and represented by $\sqrt{2} \cdot f$ in Fig. 13 falls outside the region of no noticeable change, which is directly proportional to the magnitude of the second-order system dynamics $|H(j\omega)|$, friction will be detected. More data from additional experiments are needed to confirm these interpretations and to determine the exact relationship between the second-order system magnitude response and the detection threshold in friction. So where current results show a connection between $|H(j\omega)|$ and friction JND, which are best explained by a change in detection *threshold* of friction, how this change in detection threshold occurs can only be hypothesized on.

Revisiting the main research question, formulated in the Introduction, our findings show that mass–spring–damper dynamics can indeed have a masking effect on the perception of differences in friction. Under conditions where the ratio of friction to $|H(j\omega)|$ is sufficiently large, JNDs in friction may follow

Weber's law. The Weber fractions of around 20% are close to what has been found for the tactile perception of friction in isolation [18], suggesting that these findings may be more universally applicable and not only to perceiving changes in dynamics by means of a side-stick controller. When considering the requirements of haptic feedback transparency of the CLS in flight simulator training, as set by the European Union (EASA) [6] and U.S. aviation safety agencies (FAA) [7], the findings presented here can be combined with Fu's JND model to establish a more human-centric approach in regulating CLS transparency.

In future research, the results of this study have to be replicated, while performing more focused experiments. Furthermore, the second research question as formulated in the Introduction of how friction affects JNDs in $\Re H(j\omega)$ and $\angle H(j\omega)$ should be tackled to further complement the JND model. Not knowing this effect of friction on JNDs in mass, stiffness, and damping, however, does not make the JND model less usable. It will just be more conservative, as potential masking effects are not taken into account. Therefore, it is possible to start applying the human-centric design of haptic interfaces using an incomplete JND model, realizing that, since that the current model should be considered conservative, this would also lead to a conservative design of the interfaces.

A new question that this research raises is what the detection threshold for friction is and how it behaves in the presence of second-order dynamics. This study shows that the detection threshold for friction can be influenced by mass–spring–damper dynamics, which in turn affect the Weber fractions, illustrated in Fig. 12. To fully model JNDs in friction in the presence of second-order dynamics it might be necessary to also construct a model of friction detection thresholds, including, again, the potential effects of mass–spring–damper dynamics.

VI. Conclusion

It is investigated whether the perception of friction can be masked by mass–spring–damper dynamics, and if so how the threshold for perceiving friction changes is affected by these dynamics. Experimental results suggest that JNDs in friction follow Weber's law, also in the presence of second-order system dynamics, but *only* when the level of friction is sufficiently large compared to the system impedance. While JNDs in friction are a constant proportion of reference friction, at the limits of perception Weber's law breaks down, causing larger JNDs. How close a particular level of friction is to the perception limit can be established from the ratio of friction to the system magnitude response.

References

[1] J. G. W. Wildenbeest, D. A. Abbink, and J. F. Schorsch, "Haptic transparency increases the generalizability of motor learning during telemanipulation," in *Proc. World Haptics Conf.*, Daejeon, South Korea, 2013, pp. 707–712.

[2] T. B. Sheridan, "Telerobotics," *Automatica*, vol. 25, no. 4, pp. 487–507, 1989.

[3] S. Avgousti et al., "Medical telerobotic systems: Current status and future trends," *BioMed Eng. OnLine*, vol. 15, no. 1, pp. 1–44, 2016.

[4] T. Fong, J. Zumbado, N. Currie-Gregg, A. Mishkin, and D. L. Akin, "Space telerobotics: Unique challenges to human-robot collaboration in space," *Rev. Hum. Factors Ergonom.*, vol. 9, pp. 6–56, 2013.

[5] N. Dahlstrom, S. W. A. Dekker, R. Winsen, and J. Nyce, "Fidelity and validity of simulator training," *Theor. Issues Ergonom. Sci.*, vol. 10, no. 4, pp. 305–314, 2009.

[6] Anon., "CS-FSTD(A): Certification specifications for aeroplane flight simulation training," EASA, Tech. Rep. CS-FSTD(A), 2018.

[7] Anon., "14 CFR part 60: Flight simulation training device initial and continuing qualification and use," FAA, Tech. Rep. 14 CFR Part 60, 2016.

[8] R. W. Daniel and P. R. McAree, "Fundamental limits of performance for force reflecting teleoperation," *Int. J. Robot. Res.*, vol. 17, no. 8, pp. 811–830, 1998.

[9] E. H. Weber and D. Pulsu, *Resorptione, Auditu et Tactu: Annotationes Anatomicae et Physiologicae*. Leipzig, Germany: CF Koehler, 1834.

[10] G. T. Fechner, *Elemente der Psychophysik*. Leipzig, Germany: Breitkopf and Härtel, 1860.

[11] L. A. Jones and I. W. Hunter, "A perceptual analysis of stiffness," *Exp. Brain Res.*, vol. 79, pp. 150–156, 2004.

[12] L. A. Jones and I. W. Hunter, "A perceptual analysis of viscosity," *Exp. Brain Res.*, vol. 94, pp. 343–351, 2004.

[13] M. Rank, T. Schauß, A. Peer, S. Hirche, and R. L. Klatzky, "Masking effects for damping JND," in *Haptics: Perception, Devices, Mobility, and Communication*, P. Isokoski and J. Springare, Eds. Berlin, Germany: Springer, 2012, pp. 145–150.

[14] W. Fu, A. Landman, M. M. van Paassen, and M. Mulder, "Modeling human difference threshold in perceiving mechanical properties from force," *IEEE Trans. Hum.- Mach. Syst.*, vol. 48, no. 4, pp. 359–368, Aug. 2018.

[15] W. Fu, M. M. van Paassen, D. A. Abbink, and M. Mulder, "Framework for human haptic perception with delayed force feedback," *IEEE Trans. Hum.- Mach. Syst.*, vol. 49, no. 2, pp. 171–182, Apr. 2019.

[16] W. Fu, M. M. van Paassen, and M. Mulder, "Human threshold model for perceiving changes in system dynamics," *IEEE Trans. Hum.- Mach. Syst.*, vol. 50, no. 5, pp. 444–453, Oct. 2020.

[17] W. Fu, personal communication [email]. 2021.

[18] D. Gueorguiev, E. Vezzoli, A. Mouraux, B. Lemaire-Semail, and J.-L. Thonnard, "The tactile perception of transient changes in friction," *J. Roy. Soc. Interface*, vol. 14, 2017, Art. no. 20170641.

[19] W. Ben Messaoud, M.-A. Bueno, and B. Lemaire-Semail, "Relation between human perceived friction and finger friction characteristics," *Tribol. Int.*, vol. 98, pp. 261–269, 2016.

[20] O. Caldiran, H. Z. Tan, and C. Basdogan, "Visuo-haptic discrimination of viscoelastic materials," *IEEE Trans. Haptics*, vol. 12, no. 4, pp. 438–450, Oct.–Dec. 2019.

[21] E. Samur, J. E. Colgate, and M. A. Peshkin, "Psychophysical evaluation of a variable friction tactile interface," *Proc. SPIE*, vol. 7240, pp. 167–173, 2009.

[22] W. Tang, R. Liu, Y. Shi, C. Hu, S. Bai, and H. Zhu, "From finger friction to brain activation: Tactile perception of the roughness of gratings," *J. Adv. Res.*, vol. 21, pp. 129–139, 2020.

[23] Y. Liu, J. Li, Z. Zhang, X. Hu, and W. Zhang, "Experimental comparison of five friction models on the same test-bed of the micro stick-slip motion system," *Mech. Sci.*, vol. 6, pp. 15–28, 2015.

[24] P. R. Dahl, "A solid friction model" Space Missile Syst. Organisation, Air Force Syst. Command, El Segundo, CA, USA, Tech. Rep. SAMSO-TR-77-131, 1968.

[25] K. Johanastrom and C. Canudas-de Wit, "Revisiting the LuGre friction model," *IEEE Control Syst. Mag.*, vol. 28, no. 6, pp. 101–114, Dec. 2008.

[26] W. Fu, M. M. van Paassen, and M. Mulder, "The influence of discrimination strategy on the JND in human haptic perception of manipulator stiffness," in *Proc. AIAA MST Conf.*, Denver, USA, 2017, p. 3668.

[27] K. H. Norwich, "On the theory of Weber fractions," *Percep. Psychophys.*, vol. 42, pp. 286–298, 1987.

[28] F. Kingdom and N. Prins, *Psychophysics: A Practical Introduction*, 2nd ed. San Diego: Academic Press, 2016.